# Equipment, Material and Processes for UV-DLP- Based Additive Manufacturing of Two-Component Ceramic Green Bodies and Dense Structures

Patrick Springer*[1], Eric Schwarzer*[2], Oliver Refle[1], Hans-Jürgen Richter[2]

[1] Fraunhofer IPA, Stuttgart, Germany
[2] Fraunhofer IKTS, Dresden, Germany

* Corresponding Author: patrick.springer@ipa.fraunhofer.de, eric.schwarzer@ikts.fraunhofer.de

*Abstract*

*In medical as well as technical applications, multi-material ceramic structures can be used to realise enhanced solutions with integrated functionalities. This paper introduces a modular machine design, specifically developed photosensitive ceramic based ($ZrO_2$) slurry materials, and processes to produce green bodies consisting of two slurry materials in an automated process flow. In manual tests single- and multi-material structures consisting of the developed slurry materials were laminated to determine whether it was possible to manufacture dense green bodies and sintered ceramics in a layer wise approach. Furthermore complex mono-material green bodies were manufactured using the developed test stand with an automated process flow. Subsequently, green bodies were sintered to dense ceramic components. Based on these results simple bi-material green bodies have been produced using contactless industry standard dispensing technology to demonstrate the feasibility of the approach. It has been shown that this Additive Manufacturing (AM) approach is capable of producing complex single material green bodies which have been sintered to dense ceramic components (>99%) as well as simple green body structures consisting of two zirconia material variants.*

## 1 Introduction

Ceramics are high performance materials, applied in a wide range of applications. A majority of those represent complex and high-value products. Examples include medical applications such as prosthetics [1], tools for high-temperature applications [2], or dielectric substrates for sensors and measurement applications. At the same time both small lot-sizes or individualization of such components is required, while the possibilities of tooling for ceramics is limited. All these facts result in a significant need for enhanced production technologies.

AM technologies perfectly fulfil the above mentioned requirements and offer enhanced ways of producing ceramic components with increased efficiency. Added value could be provided in two manners: First, the ability to produce complex geometries efficiently and second, economical manufacturing in lot-size one. However, where the needs of products are based on the use of high-performance materials such as ceramics, there is a second aspect leading to improved capabilities: If AM processes would be further developed they could allow complex material arrangements within one single part. The ability to create so called *gradient structures* are a long-lasting promise of AM processes which have not been fulfilled despite plastic parts made of photo polymeric resins.

Transferring multi-material capabilities to ceramics, would allow for structural and functional improvements for high-value components. E.g. local adjustments of electrical or thermal conductivity would be possible as well as selectively improved mechanical properties.

This paper presents equipment-, material- and process developments to follow the illustrated goal of multi-material ceramics. In comparison to state of the art, the material application process of each layer is done locally selective to establish a new AM approach capable of building multi-material ceramics.

## 2 State-of-the-art Processes and Materials for Additive Manufacturing of ceramics

### 2.1 Additive Manufacturing technologies for ceramics

AM processes can be very suitable for the production of ceramic green bodies. This section clusters and partially introduces state-of-the-art AM technologies and focuses on commercially available systems.

The basis for clustering AM technologies is determined by the ISO/ASTM 17296 standard. Deckers et al. [3] presented a comprehensive overview over the current state of AM technologies and applications. Specialist books such as [4–6] provide a comprehensive overview of the different AM processes.

In terms of the production of ceramic components two routes can be distinguished: (1) single- and (2) multi-step approaches. Single-step processes such as directenergy deposition and powder bed fusion allow for direct manufacturing of ceramic components without a subsequent, separate debinding and sintering step. Therefore these processes are very fast but mostly used for production of porous components. This section will focus on multi-step processes which require a subsequent furnace treatment for the debinding and sintering of AM produced green body structures. This more time consuming approach allows for the manufacturing of components with densities of up to 98% as well as tensile and flexural strength values of 327 and 472 MPa for alumina components [7]. The linear shrinkage between the green body and sintered state during debinding and sintering is different for each process and is in the range of 18-30% [8, 9].

The most common AM technology used for manufacturing of ceramic green bodies incl. recent references of the processes and applications are:

- (Direct) Inkjet Printing [8]
- Material Extrusion [10]
- Binder Jetting [11]
- Powder Bed Fusion [12]
- Vat Photopolymerization / Stereolithography (STL) [9, 13]

Since this paper uses a DLP-based stereolithographic approach this process is described in further detail in the following section.

### 2.2 Slurry-and DLP-based Additive Manufacturing ceramic green body manufacturing

As previously mentioned the slurry and DLP-based manufacturing approach is promising in terms of the production of high performance ceramic components.

The most common process uses a DLP projector combined with a light source in a wavelength of 365-465 nm for the flat as well as local resolute layer-by-layer polymerization in a component. Based on DLP, Lithoz GmbH developed an AM process called lithography-based ceramic manufacturing (LCM) and the first commercially available machine for the production of technical, dense ceramics with good surface quality and resolutions up to 635 dpi [14–17]. Furthermore, a compatible system has been introduced by Admatec, Netherlands.

Another system has been developed by Prodways, France. Here, vats are illuminated from by movable DLP units. The building tray is lowered into the vat layerwise and a doctor blade is used to level the liquid surface. The well-known slurry producer 3DCeram, France develops UV-curable, ceramic based suspensions and manufactures ceramic green bodies by UV-laser technology.

### 2.3 Multi-Material Processing

In terms of manufacturing multi-material ceramic green body structures via UV-curable, ceramic based slurries there are no recent publications. The proof of feasibility of multi-material processing with polymers has been given e.g. by Choi et. al. [18]. The process consisted of manually removing a vat, draining the current material, rinsing the vat, returning the vat to the system, and finally dispensing a prescribed volume in the vat using a syringe pump. By this means, three-dimensional pure polymeric structures have been manufactured.

### 2.4 Additive Manufacturing processable slurry materials

Today, AM technologies which process polymers are state-of-the-art [19, 19–21]. One of the best-known AM technologies is the conventional stereolithographic process (STL), established for polymers and now applied for alumina [22], zirconia, silicon nitride as well as for silica [23]. Selective photo polymerization of UV curable organics or inks (resin-based acrylate or water-based acrylamide) is the basis of the STL-process. 3DCeram, a well-known company with expertise in Laser-STL for more than 10 years, developed a material portfolio including alumina, zirconia hydroxyapatite, mullite and cordierite, which covers a wide range of applications. [24] However, one deficit of the process is the large bulk of materials, which is needed in the building area during the manufacturing process. To date, Lithoz offers a product portfolio of three materials - an alumina, a zirconia and a hydroxyapatite suspension.

## 3 Experimental Setup

### 3.1 Manual Device for Manufacturing of simple Multilayer structures

To characterise the rheological as well as the polymerization behaviour of the developed zirconia suspensions a Rheometer (Modular Compact Rheometer MCR302, Anton Paar, Graz, Austria) with a cone-plate measuring system (shear rate 0-100 $s^{-1}$) and a plate-plate-system combined with a light source (Omnicure, 300-500 nm wavelength) have been used.

The polymerization was characterized by measuring the complex shear modulus before and during light exposure in the MCR302 with an oscillating plate-plate measurement system (gap 100 µm, deformation of 0.1 % at 10 rad/s).

Thereafter, first simple multilayer structures consisting of the developed suspensions were manufactured layer-by-layer to investigate the shaping and interconnection between layers within the green and sintered state.

Therefore, an apparatus using a metallic doctor-blade and suitable frames with a thickness of 100 µm was manufactured, as shown Figure 1.

Figure 1 shows the manufacturing process of simple multilayer compounds. The device uses a doctor blade to streak the suspension within the frame to create single layers (I-II). The layers are solidified with a UV-light source (III) and the frame is raised to host the next layer (IV). This method creates multi-layered components of the zirconia suspensions and in a next step, combinations of two suspensions in one component to show the possibility of mixed structures. The manual shaped multi-layered structures were debindered and sintered subsequently.

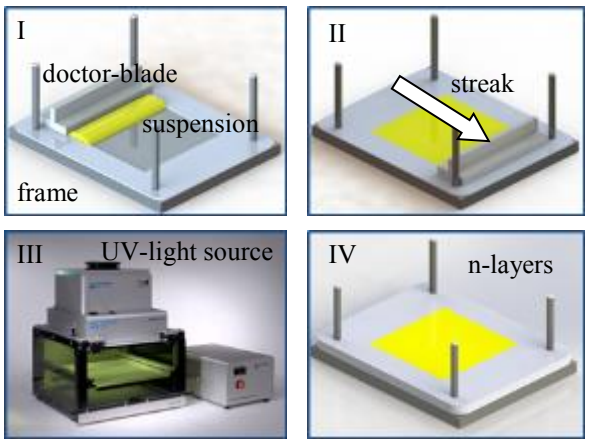


*Figure 1: schematic view of the stepwise (I-IV) manufacturing of simple multilayer zirconia structures*

### 3.2 Modular Machine Concept

A modular, completely automated test rig has been designed and set up which consists of two main linear axis which carry different process modules. Figure 2 shows the general layout of the machine which consists of: (I) Dispensing and smoothing unit, (II) Ink-Jet unit and (III) space for modular building chambers. The linear axis (I) can host different process modules such as (IV) a x-y tray table for dynamic movement of dispensing units as well as a smoothing module. These modules can be moved above the build area and use an experimental setup as described in more detail in the following paragraphs.

*Dispensing Module*

To be able to apply slurry material selectively two identical dispensing valves of the type Nordson EFD PICO xMOD, nozzle diameter 100 µm were used. The system used zirconia sealing components and was able to jet highly viscous and particle filled suspensions at high frequencies (500 Hz). This system can apply slurry materials in minimal quantities without contact to the surface.

As shown in Figure 2 (IV), the dispensing valves were mounted on an x-y-tray portal, which dynamically executes NC-code commands. By this means, slurry material can be applied selectively on the building area.

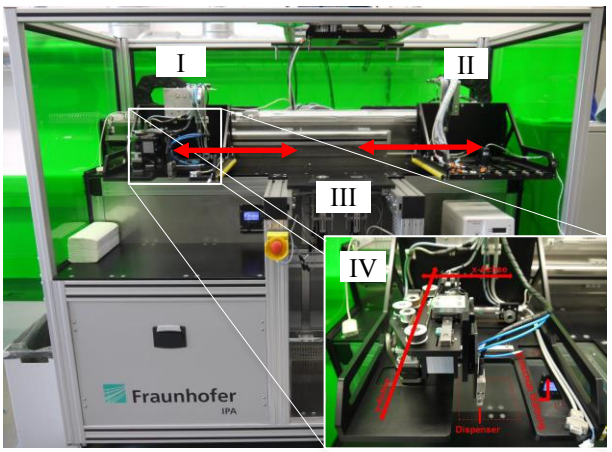


*Figure 2: Setup test rig including dispense axis (I), Ink-Jet axis (II), modular building area (III) and detailed view of x-y-portal for dispensing (IV).*

*Smoothing Module*

A smoothing module using a stainless steel roller was developed and was used as a doctor roller (Figure 3). Since two or more slurry materials can be processed, the roller operates in counter rotation to actively dispatch surplus material. By this means, the layer thickness (10-100 µm) is controlled effectively and the liquid surface is smoothed. Waste material is removed by a peristaltic pump and a hose system.

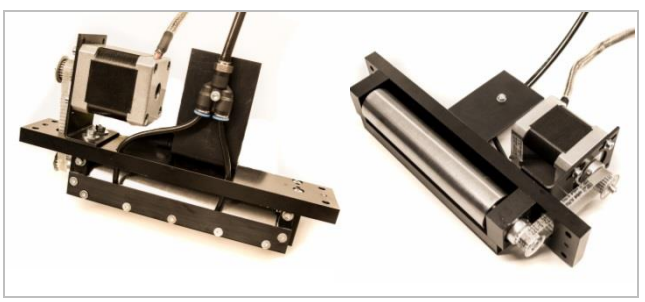

*Figure 3: Specifically developed smoothing unit using a stainless steel roller: front view (left), back view with slurry suction unit (right).*

*UV-DLP Module*

To selectively solidify the UV curable slurry materials a ViALUX DLP (HP-LED-OM-095) Module with specifically designed optics, Full-HD resolution (1080 x 1920 px) and a resulting focused pixel size of 50x50 µm is used. The projector is equipped with a 10 W LED-UV light source with a wavelength of 375 nm which allows a radiometric flux in projected field of >1W. The module was mounted on a pneumatically driven linear axis (not shown in Figure 3) directly above the build area. It can be lowered and

centred above the build area at both specific and adjustable heights.

## 4 Results and Discussion

In this study, two different light curable zirconia (ZrO2) suspensions (slurries) were developed and used to create mono- as well as bi-materials components. In the first step green bodies and sintered ceramics were manufactured with the developed suspensions in a manual way using the apparatus introduced in section 3.1. In a second step tooth-like mono-material structures and simple bi-material structures were produced using the automated test stand introduced in section 3.2.

As an example application dental shapes consisting of different materials in one structure - an opaque core and a translucent shell in one component - were chosen to obtain the optical effect of natural teeth. Therefore, different material systems were required, in order to accomplish different boundary conditions – (1) similar AM processing properties like rheological behaviour, (2) the same sintering behaviour to avoid defects and (3) different optical requirements in the sintered structure.

### 4.1 Development of Zirconia based Suspensions

Two zirconia materials, s-type and se-type, were used for the suspensions of the developed DLP-based AM process. For the preparation of the suspensions, the different stabilized zirconia materials (powder content of 30-vol%) containing 3-mol% $Y_2O_3$ were dispersed in a reactive diluter (acrylicacidester) by ball milling for 4 hours together with a dispersing agent (aliphatic polyether with acidic groups). The used binder system consists of an UV-curable polymer/oligomer (amin-modified polyetheracrylate) and a photoinitiator (phenyl-phosphineoxide) activated at 360-380 nm wavelength. After preparation the suspensions were characterized regarding particle size distribution and rheological as well as solidification behaviour during light exposure.

Since the rheological behaviour of the suspensions is crucial for the jetting process during printing, the characterization phase is very important to evaluate the processability of the suspension. Differences in the properties of the materials such as morphology and particle diameter can be also characterized by the rheological behaviour. An ideal suspension should behave like a pseudoplastic fluid in a low viscosity range. Viscoelastic behaviour means low viscosity at high shear rates, which is important for the dispensing process and that the viscosity is high enough to fix the suspension after application. Another important characterized property is the solidification behaviour under light exposure (800 mW/cm² at 300-500 nm wavelengths).

During the experiments, two photo-curable suspensions using a zirconia s-type and se-type, in a particle content of 30-vol%, were developed and characterized. Table 1 shows the basic properties of the two suspensions.

*Table 1: zirconia materials and their properties*

| $ZrO_2$-type | $d_{50}$ [µm] | $A_O$ [µm] | optical property |
|---|---|---|---|
| S | 0.45 | 7.2 | translucent |
| SE | 0.59 | 6.8 | opaque |

The s-type suspension for the translucent parts recorded a smaller particle size of $d_{50}$= 0.45 µm against the se-type with a particle size $d_{50}$= 0.59 µm used for opaque parts. Due to this, differences in the rheological behaviour and the polymerization were possible. The rheological behaviour of the suspensions is compared as a plot of viscosity vs. shear-rate, as shown in Figure 4.

Both curves show a pseudo-plastic behaviour usable in the AM process. Because of the lower particle size of the se-type suspension, the viscosity is lower. For both suspensions, the viscosity is smaller than 5 Pa*s at a shear rate of 10 $s^{-1}$ and therefore jetting the suspension using the introduced dispensing technology is possible.

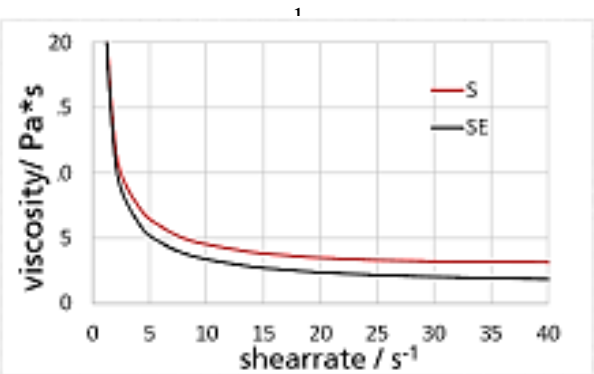


*Figure 4: viscosity over shear rate for photo curable s- and se-type suspension*

The polymerization has been characterised and the result is shown in Figure 5, given by the plot of the storage modulus (G´) and the first derivation of G´ vs. time. Before starting polymerization by light exposure the suspensions behave like viscoelastic fluids with constant G´ smaller than one MPa. The light exposure starts at 70 s and the polymerization begins because the G´ as well as the strength of the suspension is rising up to 1300 MPa, which show the end of solidification. Polymerization of the s-type suspension starts slow compared to the se-type, and can be calculated as the difference between the beginning and end of the slope.

Due to the smaller particle of the se-type suspension, the polymerization time is approximately 30 s and for the s-type 25 s, both times are acceptable for the processing.

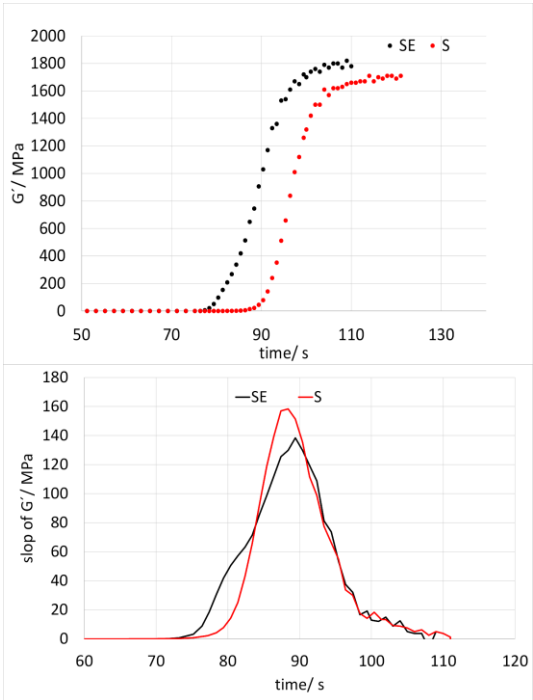


*Figure 5: storage modulus G´ (left) and slope of G´ (right) vs time during light exposure (1.5 W/cm²)*

### 4.2 Solidification and layer formation

For the production and principal validation of single- and multilayer structures the previously introduced manual metallic doctor-blade apparatus (see Figure 1) was used. Examples are given in Figure 6.

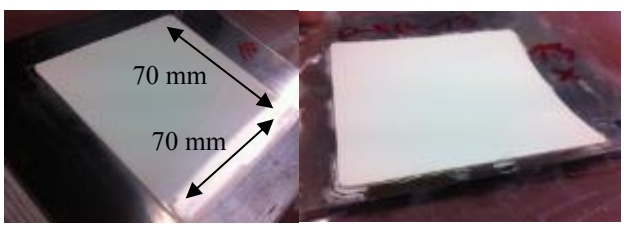


*Figure 6: ten layers of a component after light exposure (left) and 13 layers without frames (right)*

Following, the production of the multilayer structure and the quality of the substrates was visually analysed. The removal of the metal frame caused delamination at the edges of the substrates. Altogether, the manufacturing of the multilayer components showed an acceptable result and the green-bodies were debindered and sintered in a next step followed by characterisation of the structure.

### 4.3 Material Application Process

The automated selective material application (dispensing) process within the introduced test rig was analysed in terms of the achievable structural resolution and regarding a closed surface dispensing.

The relevant process parameters such as cartridge pressure, slurry temperature, nozzle opening time, material drop- and line distance were analysed to produce smallest possible drops in a repeatable manner to achieve highest possible resolution. Therefore a nozzle plate with a diameter of 100 µm has been used. This study showed that the most relevant parameter was the valve opening time. The most repeatable as well as smallest achievable drops were realised with opening times of ~70 ms. The produced droplets showed a diameter of ~290 µm, see Figure 7.

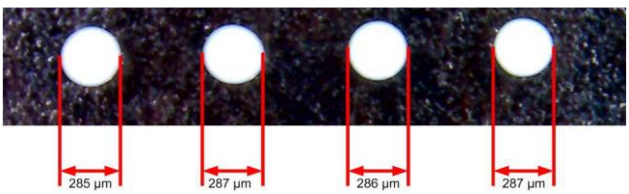


*Figure 7: Material drops with diameter of ~290 µm dispensed with 100 µm nozzle.*

This study also demonstrated that closed lines of slurry can be produced with drop distances of 200 µm. Furthermore closed surfaces of dispensed slurry material can be achieved with line distances of 250 µm. Within the experiment concentric circles were dispensed to investigate this effect. Figure 8 shows the result of this study with line distances of (a) 500 µm, (b) 400 µm, (c) 300 µm and (d) 250 µm.

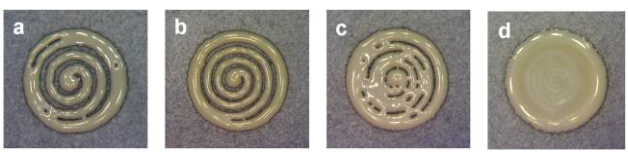


*Figure 8: Dispensed surfaces with different line distances: (a) 500 µm, (b) 400 µm, (c) 300 µm, (d) 250 mm.*

Analysis of dispensed closed areas showed an inhomogeneous surface structure in terms of height, see Figure 9 (top). To achieve smooth and homogenous surfaces as well as defined layer thicknesses the smoothing module, introduced in section 3.2 was used. The doctor roller was moved with a defined linear velocity above the building area and rotated in counter rotation to dispatch surplus material. This result is shown in Figure 9 (bottom). To guarantee the dispatch of material the peripheral speed of the doctor roller needed to be higher than the linear velocity of the module above the build area.

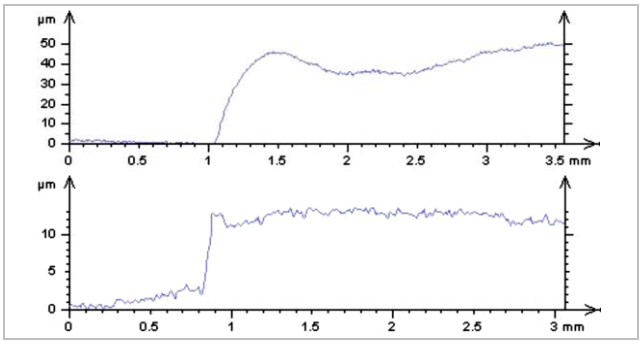


*Figure 9: Section view of (top) dispensed surface and (bottom) surface after smoothing.*

### 4.4 Green Body Manufacturing

Based on the combination of all introduced process modules, tooth like structures, such as shown in Figure 10, were produced to show the potential AM of ceramic green bodies. The illustrated part was manufactured with a layer thickness of 30 µm in $ZrO_2$. In Figure 11 a detailed top- and side view of a printed part is given which shows the layerwise structure.

The process allows layer thicknesses between 15 µm and 75 µm whereas the lower limit is given by the positioning accuracy of the vertical axis driven by a stepper motor. The upper limit is given by the DLP illumination system due to the rising level of absorption of UV light with penetration depth.

While printed geometries are connected tightly to the bottom layer or supported by suitable structures show good layer formation, geometries and bodies with undercuts that are printed without support structure tend to delaminate and produce imprecise green body structures. In an experiment, the top layer of a slurry bath was illuminated and showed a high degree of warpage within the structure due to inhomogeneous material shrinkage. To avoid effects like this, the slurry materials need a low tendency for shrinkage as well as effective support structures need to be introduced.

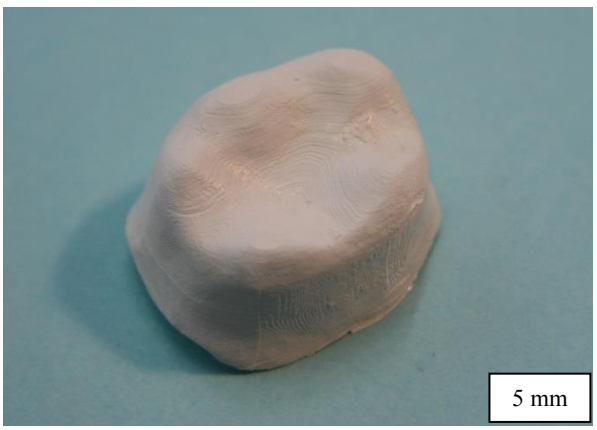


*Figure 10: Printed tooth like mono-material structure with layer height of 30 µm.*

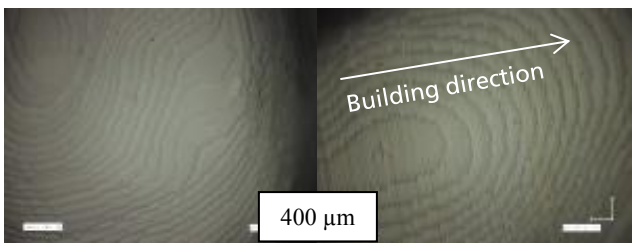


*Figure 11: Detail view of top (left) and side (right) of printed green body with layer thickness of 30 µm*

Additionally, simple two-component structures have been printed to demonstrate the feasibility of the approach. Figure 12 shows a simple printed test pattern consisting of a two zirconia variants (white and blue area) with different optical properties. To be able to visualise and distinguish the different variants the slurry materials have been coloured with smallest amounts of the colourant methylene blue (~0,005 % w/w) which has no effect on the rheological behaviour and therefore on the jetting process. Due to diffusion of the colourant between the non-solidified slurry materials, this method of visualisation is only suitable for a rough characterisation of the interface area.

Within the printing process the opaque (blue) component was applied first, while the translucent component was applied afterwards. In a second step the pattern was smoothened, levelled and subsequently solidified. To avoid material blurring through the smoothing unit the smoothing direction was chosen orthogonal to the contact zone.

Within the detailed view in Figure 12 (right) the dropwise material application approach is visible within the contact zone. The contact zone shows - even due to diffusion of the colourant - a defined and straight line and sharp interface between the two components.

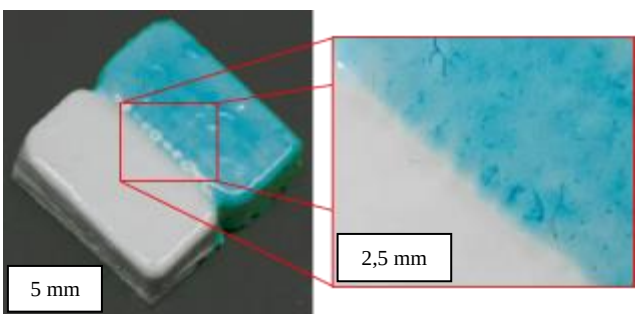


*Figure 12: Printed, bicolored two-component structure: ZrO2 – opaque (blue area, methylene blue as colourant), ZrO2 – translucent (white area)*

### 4.5 Sintered Structures

After debinding and sintering, FESEM was used to analyse the manually produced structures of the components. Figure 13 shows the structure of a multilayer, s- and se-type.

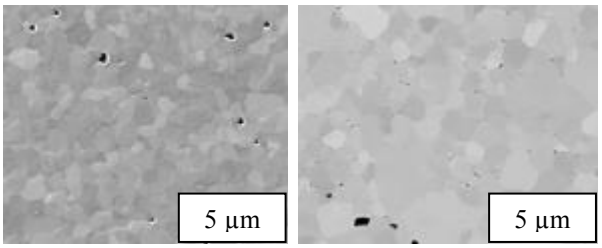


*Figure 13: sintered structure of s-(left) and se-type (right) multilayer*

The figures show the difference between the materials, because the structure of s-type is finer due to the smaller particles. Both structures have small pores caused by the processing and only small delamination points could be found. ImageJ, an open source picture-editing tool, was used for determination of porosity by calculation of the grey level in binary FESEM-pictures with the result of porosity smaller than one percent (dense > 99 %).

Figure 14 shows manually manufactured and subsequently sintered multilayer structures, first different materials inside the layers (left) and second one layer with changing materials (right).

Due to the FESEM, sintering of components with mixed suspensions is possible. Therefore, the black line shows the layer boundary between the different materials. All together the result of the manual processing shows, that

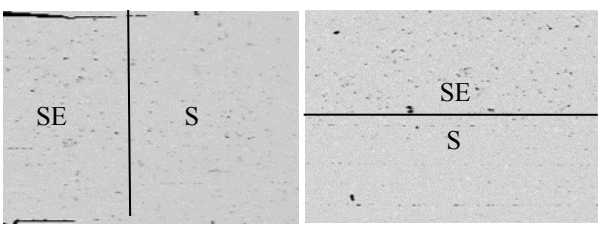


*Figure 14: suspension mixed inside of a layer (left) and changed suspension after few layers (right)*

processing of two materials in the AM dispensing process is feasible.

Finally, first simple structures manufactured by the introduced AM process approachare shown in Figure 15 and Figure 16.

The manufacturing of a star like component was the first test of processing complex structures with more than 120 layers to test the approach. Inside the structure, a low number of defects and delamination areas could be identified. The jagged/toothed edge of the structure is remarkable.This is due to light scattering effects or a non-optimized procedure. The porosity is also smaller than one percent.

Complex components like the sintered tooth like structure as shown in Figure 16, show the potential and the possibilities of the developed AM process.

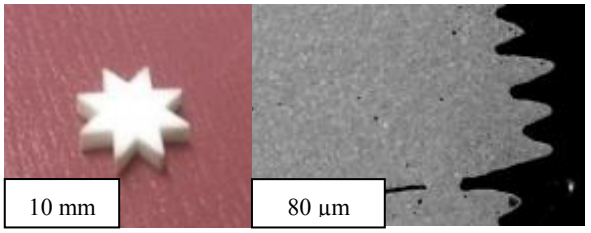


*Figure 15: AM processed star-like component (left) and sintered structure (right)*


*Figure 16: AM processed tooth like sintered structure*

## 5 Conclusion

This paper shows the development of UV curable, ceramic based slurry materials, of a modular test rig as and of processes to manufacture multi-material ceramic green bodies. Furthermore, the manufactured green bodies could have been debindered and sintered. The resulting density of the ceramic components is >90 %.

Two different photo-curable suspensions of $ZrO_2$ compatible with a new AM approach based on DLP- and dispensing-technologies were developed and characterized regarding their rheological and polymerization behaviour. Thereby, the suspensions show similar properties with minor differences regarding flow behaviour as well as polymerization kinetic. Nevertheless, the preparation of suspensions needs to be optimized for a high quality structure. Effects such as shrinkage during solidification need to be optimised, to lower the effects of warpage and delamination on the manufactured green bodies.

The essential functionality of the developed slurry material for DLP-based Additive Manufacturing has been proven using manually laminated single- and multi-material compounds.

A specifically designed and fully automated, modular test rig as well as adapted process flows have been developed. On this basis, complex single material green body structures have been produced in additive manufacturing and sintered to pure ceramic

components. Simple bi-material green body structures proof the feasibility to manufacture multi-material ceramics by the introduced approach. However, problems have been identified and have to be resolved to be able to produce complex, dense, single- and multi-material ceramic components in an economical manner.

Using the introduced AM approach to produce single material components, several problems occurred during printing. Warpage of unsupported layers and structures lead to inaccurate green body structures and need to be minimised. Therefore, slurries need to be optimised in terms of low shrinkage rates during solidification and effective support structures need to be identified. Furthermore, the effect of delamination needs to be minimised by adapting the process control to guarantee high density and crack free monolithic consistency of the components in sintered state. Beside this, the used dispensing system is both slow regarding the material depositioning process because of the drop wise printing approach as well as limited in terms of lifetime due to the internal sealing concept. Both problems need to be targeted with suitable application strategies.

Concerning multi material component manufacturing, the influence of the smoothing unit on the materials contact zone needs to be analysed in detail to be able to understand and control this effect. Furthermore, interdependencies between process parameters and the resulting material-interface zone need to be further investigated to be fully understood. Additionally, the investigated materials are limited to $ZrO_2$ at the moment. The range of materials needs to be increased to target technical as well as medical applications.

## Acknowledgements

This paper has been supported by Christian Seifarth (test rig design, choice of components, dimensioning and setup), Jürgen Lobe (Layout and implementation of test rig control system), Guido Frech, Mark Becker (test execution) and Markus Echsel (machine enhancement) at Fraunhofer IPA, Stuttgart.

## References

[1] W. Höland, M. Schweiger, R. Watzke, A. Peschke, and H. Kappert, “Ceramics as biomaterials for dental restoration,” (en), *Expert Review of Medical Devices*, vol. 5, no. 6, pp. 729–745, 2008.

[2] M. A. Fonseca, J. M. English, M. von Arx, and M. G. Allen, “Wireless micromachined ceramic pressure sensor for high-temperature applications,” *J. Microelectromech. Syst,* vol. 11, no. 4, pp. 337–343, 2002.

[3] J. Deckers, J. Vleugels, and J.-P. Kruth, “Additive Manufacturing of Ceramics: A Review,” (af), *Journal of Ceramic Science and Technology*, no. Vol.5, No.4, pp. 245–260, 2014.

[4] I. Gibson, D. W. Rosen, and B. Stucker, *Additive Manufacturing Technologies: Rapid Prototyping to Direct Digital Manufacturing*. Boston, MA: Springer US; Springer, 2010.

[5] A. Bandyopadhyay and S. Bose, *Additive manufacturing*. Boca Raton: CRC Press, 2015.

[6] A. Gebhardt, *Generative Fertigungsverfahren: Additive Manufacturing und 3D Drucken für Prototyping ; Tooling ; Produktion,* 1st ed. München: Carl Hanser Verlag, 2013.

[7] J.-C. Wang, “A novel fabrication method of high strength alumina ceramic parts based on solvent-based slurry stereolithography and sintering,” (English), *International Journal of Precision Engineering and Manufacturing*, vol. 14, no. 3, pp. 485–491, http://dx.doi.org/10.1007/s12541-013-0065-3, 2013.

[8] J. Ebert, E. Özkol, A. Zeichner, K. Uibel, O. Weiss, U. Koops, R. Telle, and H. Fischer, “Direct Inkjet Printing of Dental Prostheses Made of Zirconia,” (en), *Journal of Dental Research*, vol. 88, no. 7, pp. 673–676, 2009.

[9] T. Chartier, A. Badev, Y. Abouliatim, P. Lebaudy, and L. Lecamp, “Stereolithography process: Influence of the rheology of silica suspensions and of the medium on polymerization kinetics – Cured depth and width,” (en), *Journal of the European Ceramic Society*, vol. 32, no. 8, pp. 1625–1634, 2012.

[10] K. Cai, B. Román-Manso, J. E. Smay, J. Zhou, M. I. Osendi, M. Belmonte, P. Miranzo, and H.-J. Kleebe, “Geometrically Complex Silicon Carbide Structures Fabricated by Robocasting,” *J. Am. Ceram. Soc,* vol. 95, no. 8, pp. 2660–2666, 2012.

[11] H. Seitz, W. Rieder, S. Irsen, B. Leukers, and C. Tille, “Three-dimensional printing of porous ceramic scaffolds for bone tissue engineering,” (eng), *J Biomed Mater Res Part B Appl Biomater*, vol. 74, no. 2, pp. 782–788, 2005.

[12] K. Shahzad, J. Deckers, J.-P. Kruth, and J. Vleugels, “Additive manufacturing of alumina parts by indirect selective laser sintering and post processing,” *Journal of Materials Processing Technology*, vol. 213, no. 9, pp. 1484–1494, 2013.

[13] Z. Chen, D. Li, and W. Zhou, “Process parameters appraisal of fabricating ceramic parts based on stereolithography using the Taguchi method,” *Proceedings of the Institution of Mechanical Engineers, Part B: Journal of Engineering Manufacture*, vol. 226, no. 7, pp. 1249–1258, 2012.

[14] C. W. Hull, "Apparatus for production of three-dimensional objects by stereolithography", US 63890584, March 11, 1986

[15] J. Homa and M. Schwentenwein, “A Novel Additive Manufacturing Technology for High-Performance Ceramics,” *Ceramic Engineering and Science Proceedings*, vol. 6, no. 35, pp. 33–40, 2014.

[16] R. Felzmann, S. Gruber, G. Mitteramskogler, P. Tesavibul, A. R. Boccaccini, R. Liska, and J. Stampfl, “Lithography-Based Additive Manufacturing of Cellular Ceramic Structures,” (af), *Adv. Eng. Mater,* vol. 14, no. 12, pp. 1052–1058, 2012.

[17] S. Gruber, J. Stampfl, R. Felzmann, and S. Springer, “Lithographiebasierte Fertigung keramischer Bauteile,” Aufsatz, Institut für Werkstoffwissenschaften und Werkstofftechnologie, Technische Universität Wien, Wien, 2011.

[18] J.-W. Choi, H.-C. Kim, and R. B. Wicker, “Multi-material stereolithography,” *Journal of Materials Processing Technology*, vol. 211, no. 3, pp. 318–328, 2011.

[19] M. Hofmann, “3D Printing Gets a Boost and Opportunities with Polymer Materials,” *ACS Macro Lett,* vol. 3, no. 4, pp. 382–386, 2014.

[20] R. D. Goodridge, C. J. Tuck, and R. Hague, “Laser sintering of polyamides and other polymers,” *Progress in Materials Science*, vol. 57, no. 2, pp. 229–267, 2012.

[21] L. E. Murr, E. Martinez, K. N. Amato, S. M. Gaytan, J. Hernandez, D. A. Ramirez, P. W. Shindo, F. Medina, and R. B. Wicker, “Fabrication of Metal and Alloy Components by Additive Manufacturing: Examples of 3D Materials Science,” *Journal of Materials Research and Technology*, vol. 1, no. 1, pp. 42–54, 2012.

[22] K. Pham-Gia, W. Rossner, B. Wessler, M. Schäfer, and M. Schwarz, “Rapid prototyping of high density alumina ceramics using stereolithography,” *Ceramic Forum International*, vol. 13, no. 83, pp. 36–40, 2006.

[23] A. Licciulli, C. Corcione, A. Greco, V. Amicarelli, and A. Maffezzoli, “Laser stereolithography of ZrO2 toughened Al2O3,” *Journal of the European Ceramic Society*, vol. 24, no. 15-16, pp. 3769–3777, 2004.

[24] 3D Ceram, *Homepage 3D Ceram.* Available: http://3dceram.com/de/ (2015, Nov. 19).